LINES OF CIRCUMSTELLAR C_2, CN, AND CH^+ IN THE OPTICAL SPECTRA OF POST-AGB STARS

ERIC J. BAKKER AND DAVID L. LAMBERT
Department of Astronomy and McDonald Observatory
University of Texas, Austin TX, U.S.A.

AND

EWINE F. VAN DISHOECK
Leiden Observatory, University of Leiden, The Netherlands

Abstract. Recent optical spectra of post–AGB stars show the presence of C_2, CN, and CH^+ originating in the circumstellar shell. We present here new, higher resolution spectra which provide constraints on the physical parameters and information on the line profiles. An empirical curve of growth for the C_2 Phillips and CN Red system lines in the spectrum of HD 56126 yields $b = 0.50^{+0.59}_{-0.23}$ km s^{-1}. CH^+ (0,0) emission lines in the spectrum of the Red Rectangle have been resolved with a FWHM $\approx 8.5 \pm 0.8$ km s^{-1}. The circumstellar CN lines of IRAS 08005–2356 are resolved into two separate components with a velocity separation of $\Delta v = 5.7 \pm 2.0$ km s^{-1}. The line profiles of CN of HD 235858 have not been resolved.

1. Introduction

Post–AGB stars are in a transition stage between the Asymptotic Giant Branch (AGB) and the planetary nebulae (PN) stage. During the early stage of post–AGB evolution the star is obscured by material expelled during the AGB phase (the AGB ejecta). As this ejecta slowly moves away from the central star, the optical depth decreases and the star can be detected in the optical region. When the star reaches high enough temperatures, the AGB ejecta is ionized and is observable as a planetary nebula.

We have studied optically bright post–AGB stars (spectral type A to G supergiants) which show circumstellar molecular line absorption (C_2 and CN, or CH^+) or emission (CH^+) in their optical spectra. The radial velocities and low excitation temperatures of the molecules (Bakker et al. 1996,

R.F. Wing (ed.), The Carbon Star Phenomenon, 217-224.

1997) identify them as circumstellar rather than photospheric or interstellar (see also Hrivnak 1995). The excitation of C_2 is generally described by rather high temperatures, $T_{ex} = 43 - 399$ K, whereas the CN excitation is found to be much lower, $18 - 50$ K. The reason for this difference is discussed in section 2.2. The observed abundances and excitation of the molecules can lead to a determination of the mass-loss rate.

We have used the C_2 ($A^1\Pi_u - X^1\Sigma_g^+$) and CN ($A^2\Pi - X^2\Sigma^+$) data of HD 56126 to study optical depth effects by means of the curve of growth, and we present the first results of a survey to observe these optical molecular bands at high spectral resolution ($R \geq 120\,000$). Our primary goal is to resolve the line profiles and to determine the Doppler parameter b and the chemical (e.g. abundances) and physical (e.g. expansion velocities and temperatures) conditions of the circumstellar shell.

2. Curve of Growth Analysis for HD 56126

2.1. THE EMPIRICAL CURVE OF GROWTH

A curve of growth (CoG) has been empirically determined for the $^{12}C^{12}C$ Phillips ($A^1\Pi_u - X^1\Sigma_g^+$) ($v' = 1, 2, 3$, $v'' = 0$, $J'' \leq 24$) and the $^{12}C^{14}N$ Red system ($A^2\Pi - X^2\Sigma^+$) bands ($v' = 1, 2, 3$, $v'' = 0$, $N'' \leq 3$) of HD 56126 (Figure 1). Our motive for this investigation is to decide whether the assumption of optically thin lines for the weaker bands (e.g. 3,0) is valid. The equivalent widths are taken from the work of Bakker et al. (1996, 1997). The range of line oscillator strengths is 6.67×10^{-5} to 1.44×10^{-3} and 7.19×10^{-5} to 9.79×10^{-4} for C_2 and CN, respectively.

Because three C_2 Phillips bands have been observed, the CoG has for each lower energy level J'' up to nine transitions (a P, Q, and R branch for each band). This redundancy allows the determination of the CoG. All transitions from a given J'' level are fitted to the CoG by changing the column density of that level $N(J'')$. For the CN Red system the redundancy is higher due to spin-doublet splitting of the lower and upper electronic state and Λ-type doubling of the upper electronic state. There are twelve transitions from each N'' level: six main and six satellite branches. Three bands were used, which gives in total 36 allowed transitions per N'' level (F_1 and F_2).

After all observed J'' (or N'') levels have been fitted to the CoG (Fig. 1, left panels) an optical-depth-corrected absolute rotational diagram (Fig. 1, middle panels) gives the absolute population for each J'' (or N'') level. Under the assumption of a Boltzmann distribution, a linear fit to the diagram gives the average rotational temperature T_{rot}. Finally the rotational temperature from two successive energy levels can be determined as a function

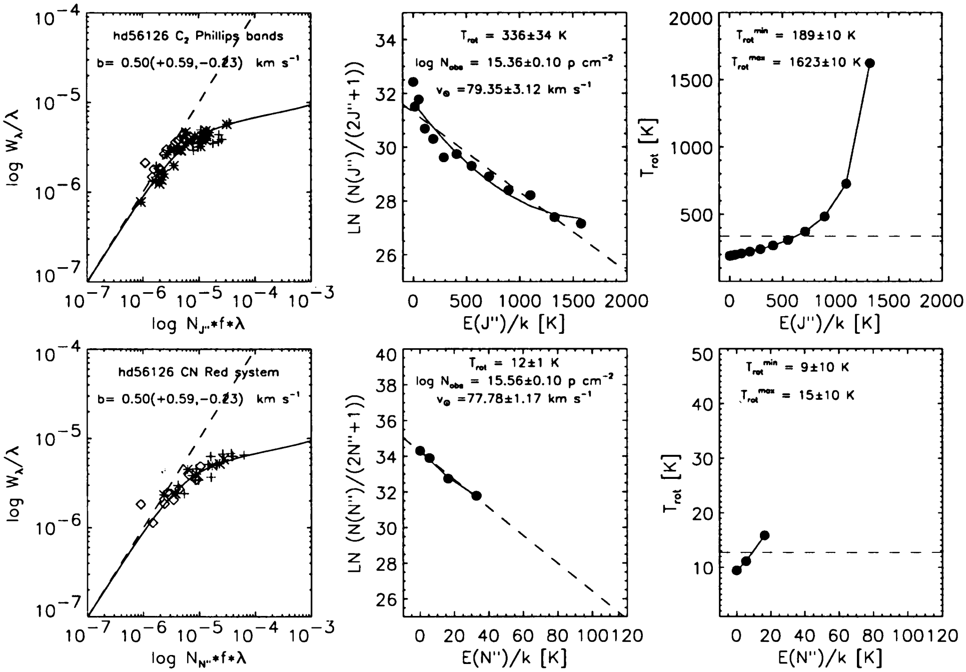

Figure 1. Curve of growth analysis for three C_2 Phillips and three CN Red system bands in the optical spectrum of HD 56126 (diamond: $v' = 3$, asterisk: $v' = 2$, plus: $v' = 1$, all for $v'' = 0$). The upper three panels concern C_2 and the lower three panels concern CN. *Left panels:* CoG with the best theoretical CoG over-plotted. *Middle panels:* optical-depth-corrected rotational diagram with a fit to the data assuming a Boltzmann distribution (dashed line) and a smooth non-Boltzmann distribution (solid line). *Right panels:* the rotational temperature determined from two successive energy levels (the dashed line is the average $T_{\rm rot}$).

of the lower energy level (Fig. 1, right panels). The parameters derived from this analysis are given in Table 1.

2.2. RESULTS AND INTERPRETATION

The empirical CoG (Fig. 1) shows clearly that the observations cover the optically-thin and saturated parts of the CoG. The theoretical CoG has a Doppler parameter $b = 0.50^{+0.59}_{-0.23}$ km s^{-1} and $\tau \approx 1$ is reached at an equivalent width of $EW(\tau \approx 1) = 18$ mÅ. Since the strongest lines in the (3,0) transitions of C_2 and CN have equivalent width of 38 and 34 mÅ, respectively, the optically thin approximation is only valid for the weaker lines in these bands. We note that all the lines of the C_2 $(v', v'') = (3,0)$ band seem to be offset with respect to the other lines. This might indicate that the band oscillator strength used is somewhat too low.

https://doi.org/10.1017/S0074180900002436 Published online by Cambridge University Press

TABLE 1. Results from the curve of growth analysis of C_2 and CN in the optical spectrum of HD 56126

	C_2 $A^1\Pi_u - X^1\Sigma_g^+$	CN $A^2\Pi - X^2\Sigma^+$	
b	0.50(+0.59, −0.23)	0.50(+0.59, −0.23)	km s^{-1}
$T_{\rm rot}$ average	336 ± 34	12 ± 1	K
$T_{\rm rot}$ minimum	189 ± 10	9 ± 10	K
$T_{\rm rot}$ maximum	1623 ± 10	15 ± 10	K
$\log N_{\rm obs}$	15.38 ± 0.10	15.56 ± 0.10	p cm^{-2}
$v_{\rm helio}$	79.35 ± 3.12	77.78 ± 1.17	km s^{-1}

The right panel of Figure 1 clearly shows that the rotational temperature for C_2 is not constant. The molecule is therefore not in local thermodynamic equilibrium (LTE) and the population distribution over the rotational energy levels is non-Boltzmann. Van Dishoeck & Black (1982) have shown that interstellar C_2 is radiatively pumped. C_2 is a homonuclear molecule and does not have allowed pure rotational or vibrational transitions and can therefore not cool radiatively: $T_{\rm rot} \geq T_{\rm kin}$. For low J'' levels the rotational temperature reaches the kinetic temperature, while for very high J'' levels the rotational temperature is expected to reach the color temperature of the local radiation field. CN on the other hand can effectively cool: $T_{\rm rot} \leq T_{\rm kin}$. Based on the population ratio between the C_2 Phillips band $J'' = 0$ and $J'' = 2$ levels we find: $T_{\rm kin} = 189 \pm 10$ K. Combining this with the derived b yields $v_{\rm microturb} = 0.34 \pm 0.6$ km s^{-1}. The measured $b = 0.50^{+0.59}_{-0.23}$ km s^{-1} gives a line profile with FWHM $= 2\sqrt{\ln 2} \times b = 0.83$ km s^{-1}. In order to resolve these lines a spectral resolution of $R \geq 360\,000$ is needed. In the presence of macroturbulence the lines are broader and can be resolved at a lower spectral resolution. The microturbulence is very likely due to a velocity gradient in the line of sight.

3. Line Profiles

3.1. CH$^+$ EMISSION LINES OF THE RED RECTANGLE

The CH$^+$ $A^1\Pi - X^1\Sigma^+$ (0,0) emission band in the optical spectrum of the Red Rectangle (HD 44179) has been observed at a resolution of $R \approx 120\,000$ using the 2.7-m telescope of McDonald Observatory (Figure 2). These lines originate from levels which are 34 000 K above the ground level. We have resolved the line profile of the strongest CH$^+$ emission lines and find a FWHM $\approx 8.5 \pm 0.8$ km s^{-1} (Table 2). The intensities of the emission lines fall below the detection limit for FWFM $\approx 20.0 \pm 1.0$ km s^{-1}. The line

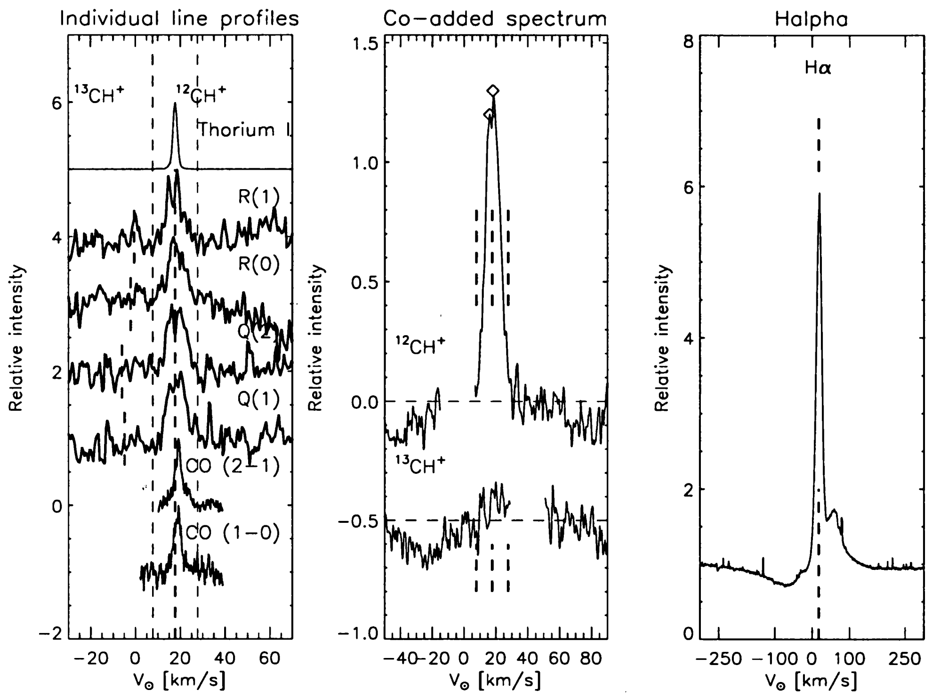

Figure 2. *Left:* normalized line profiles of the strongest CH^+ $A^1\Pi - X^1\Sigma^+$ (0,0) emission lines and CO radio emission lines (after Jura et al. 1995) of the Red Rectangle. The thick dashed lines at 17.7 km s^{-1} gives the average velocity, with on both sides (at a velocity offset of 10.0 km s^{-1}) a line where the intensity of the emission line has fallen below the detection limit. The dashed line at approximately -0.7 km s^{-1} (J'' dependent) marks the location where $^{13}CH^+$ is predicted. *Middle:* A non-detection of $^{13}CH^+$ after the signals of several lines have been co-added on a velocity axis. It seems that the $^{12}CH^+$ lines are a disk-like feature. *Right:* the Hα profile with the central spike at the system velocity.

profiles of the R(1), Q(1), and Q(2) lines suggest a central absorption or the presence of two emission components at 16.0 and 18.1 km s^{-1}. The location of $^{13}CH^+$ is at approximately -0.7 km s^{-1} (J'' dependent). To investigate the presence of weak isotopic lines we have added the signals of all lines into one single profile (middle panel of Fig. 2). We have a non-detection of $^{13}CH^+$ which yields an isotopic ratio of $^{12}C/^{13}C \geq 22$. This is consistent with the progenitor being a carbon star (Smith & Lambert 1990).

The line profile of CO is interpreted as due to a broad and narrow component (Jura et al. 1995, 1997). The broad component has a width comparable to that of the CH^+ lines which might suggest that they are formed in the same region (the circumbinary disk). The Hα and CO profiles shows a strong central emission at the system velocity. Jura et al. argue that the spike is formed in an extended region of ionized gas.

TABLE 2. Results for the Red Rectangle, HD 235858, and IRAS 08005–2356

	Red Rectangle CH^+ (0,0)	HD 235858 CN Red (2,0)	IRAS 08005–2356 CN Red (2,0)	
Date	1995 Dec. 13	1995 Sep. 17	1995 Dec. 12	
HJD	2450064.7428	2449977.6607	2450065.8708	
$v_{*,\rm helio}$	27.7 ± 1.4	-34.1 ± 0.1	64.5 ± 1.0	km s^{-1}
$v_{\rm mol,helio}$	17.7 ± 0.1	-48.2 ± 0.1	19.4 ± 0.2 (A)	km s^{-1}
			25.2 ± 1.0 (B)	
$v_{\rm FWHM}$	8.5 ± 0.8	2.2 ± 0.1	3.1 ± 0.9 (A)	km s^{-1}
			3.4 ± 2.0 (B)	
$v_{\rm FWFM}$	20.0 ± 1.0			km s^{-1}
$^{12}C/^{13}C$	≥ 22	≥ 11	≥ 11	

3.2. CN ABSORPTION IN HD 235858 AND IRAS 08005–2356

HD 235858 has been observed at a resolution of $R \approx 120\,000$. Figure 3 shows a part of the spectrum which contains three different categories of molecular features. The broad absorption lines are due to photospheric CN ($T_{\rm eff}$ = 5500 K), the narrow absorption lines are circumstellar CN ($T_{\rm eff}$ = 20 K and $\log N$ = 15.30 p cm^{-2}), and the three strongest features are telluric H_2O. There is one photospheric atomic line (N I) present in this spectrum. The circumstellar CN lines are not resolved. Since Začs et al. (1995) did not notice photospheric CN absorption in their spectrum, it seems that this pulsating star has only photospheric molecular absorption when the stellar effective temperature is sufficient low (when the star is largest).

In an earlier report on the detection of circumstellar CN in IRAS 08005–2356 we reported the presence of only one broad component (Bakker et al. 1997). The new spectra (Fig. 3, $R \approx 120\,000$) have resolved the broad component into two separate resolved components with a velocity separation of $\Delta v = 5.7 \pm 2.0$ km s^{-1}. The two absorption components could be due to wind material moving at two different velocities (multiple shells), or to two photodissociation fronts at different expansion velocities — possibly one due to the stellar and one to the interstellar radiation field.

4. Summary

We have investigated optical depth effects for the circumstellar C_2 and CN lines in the optical spectrum of HD 56126. From a curve of growth analysis we find a Doppler parameter $b = 0.50^{+0.59}_{-0.23}$ km s^{-1}. CN (2,0)

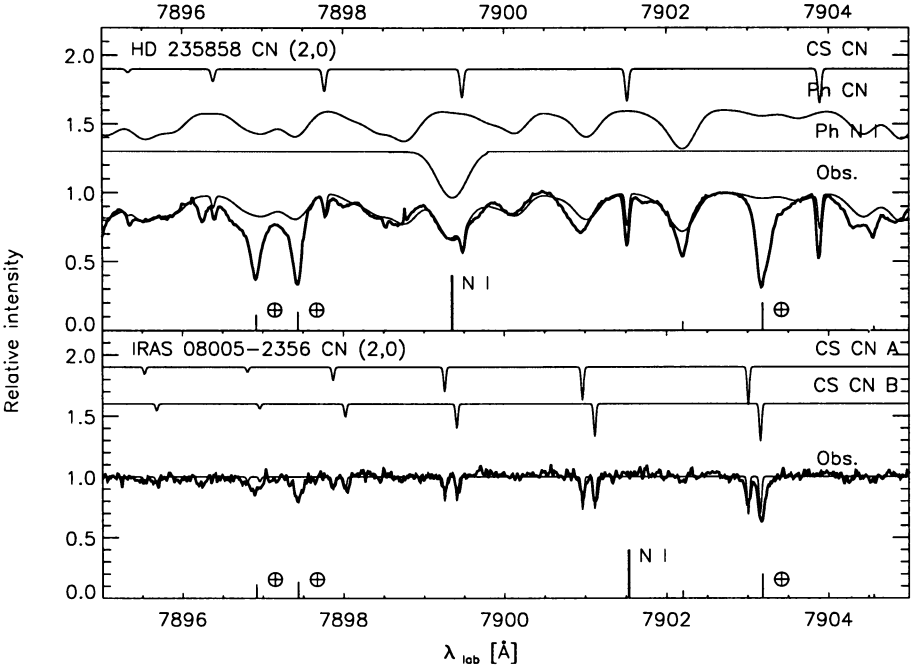

Figure 3. *Upper:* a part of the optical spectrum of HD 235858 which shows the CN Red system (2,0) band lines. *Lower:* for IRAS 08005–2356, a synthetic spectrum using photospheric and circumstellar CN lines, and N I (7898.985 Å) is over-plotted (thin line). The abscissa is in the rest frame of the molecule.

lines of IRAS 08005–2356 and HD 235858 and CH^+ of the Red Rectangle have been observed at a resolution $R \geq 120\,000$. CH^+ has been resolved. The CN lines of IRAS 08005–2356 are resolved into two separate resolved components, and the CN of HD 235858 has not been resolved.

References

Bakker, E. J., Waters, L.B.F.M., Lamers, H.J.G.L.M., Trams, N. R. & Van der Wolf, F.L.A. 1996, *A&A*, 310, 893

Bakker, E. J., van Dishoeck, E. F., Waters, L.B.F.M. & Schoenmaker, T. 1997, *A&A*, 323, 469

Hrivnak, B. J. 1995, *ApJ*, 438, 341

Jura, M., Balm, S. P. & Kahane, C. 1995, *ApJ*, 453, 721

Jura, M., Turner, J. & Balm, S. P. 1997, *ApJ*, 474, 741

Smith, V. V. & Lambert, D. L. 1990, *ApJ Supp.*, 72, 387

van Dishoeck, E. F. & Black, J. H 1982, *ApJ*, 258, 533

Začs, L., Klochkova, V. G. & Panchuk, V. E. 1995, *MNRAS*, 275, 764

Discussion

Frogel: Have you tried to observe the very strong C_2 band in the H window?

Bakker: No.

https://doi.org/10.1017/S0074180900002436 Published online by Cambridge University Press